VIBRATION TESTS AND TEST TO FAILURE OF A 7 STORIES BUILDING SURVIVED A SEVERE EARTHQUAKE

BY

Issao Funahashi*, Katsuhiro Kinoshita**
and Hiroyuki Aoyama***

ABSTRACT

Elasto-plastic behavior to failure of the Old Tokyo Marrine and Fire Insurance Building which suffered only minor damage and survided the Kanto Earthquake of September 1, 1923. (Maguitude 7.9) was investigated by static alternating loading tests and vibration tests. The objectives of these tests were to determine the stiffness, stress distribution, their changes in the plastic range, and the ultimate load carrying capacity against horizontal loads, natural period, mode and damping of vibration and finally the safety against earthquakes taking dynamic response analysis into consideration.

The stiffness of the frame as determined from test results was analyzed. The ultimate load agreed with calculated collapse mechanism as well as elastic limit. The ultimate load of 144t corresponds to the seismic shear coefficient of 0.33g. The calculated load for collapse by limit analysis was 139t. Along with the statio loading cycles, the measured period of frame increased gradually up to the final value of 1.98 sec from 0.98 sec. The damping coefficient was 3.6% for first mode, and associated with higher modes were rather small. This suggests that the damping characteristics of the frame can not be approximated by the conventional viscous damping which increases in proportion to the natural frequency.

The entire building was consisted of exterior brock masonry curtain walls and interior frame of built-up steel columns and joist girders covered with concrete. As vibration test was not carried out for the entire building, the natural periods and modes were estimated from the microtremor analysis and the structural analysis was based on the cross-section members.

The earthquake non-linear response of entire building was computed, for example El Centro Earthquake 1940 NS, 0.33g, the ductility factors at the 2nd storey were about 4 and upper stories remained in the ductility factors of 2 or less and the base shear coefficient corresponded of 0.39 respectively. Though the total absolute displacement of entire building at maximum response was shown to be 8.7cm, it was recognized that the frame remained in the elastic range by the horizontal loading test's result. As the record of Kanto earthquake was not available, the above mentioned findings may not be directly extended to actual response to Kanto Earthquake. Nevertheless, it is very interesting to note the surprising similarity to actual damages.

---

* Senior Research Officer, Takenaka Technical Research Laboratory, Tokyo
** Research Officer, Takenaka Technical Research Laboratory Tokyo
*** Associate Professor, University of Tokyo, Faculty of Engineering

VIBRATION TESTS AND TEST TO FAILURE OF A 7 STORIES BUILDING SURVIVED A SEVERE EARTHQUAKE

BY

Issao Funahashi*, Katsuhiro Kinoshita**
and Hiroyuki Aoyama

ABSTRACT

The results of an analytical and experimental investigation regarding the static and dynamic elasto-plastic characteristics of the building which suffered only minor damage and survived the Kanto Earthquake (1923, Magnitude 7.9) are described. The safety against earthquake using non-linear response analysis was studied to compared with actual damages.

Notation

The following symbols are used in this paper.

$\omega_j = \lambda_j^{\frac{1}{2}}$	resonant circular frequency of the j th mode
ψ_j	mode shape of the j th mode
h_j	percentage of critical damping of the j th mode
I	moment of inertia of foundation
$2a$	effective diameter of building which is circular
α, γ, β_1	real constant of damping
k_o, k_θ	spring constant for horizontal translation and rotation of base foundation
$G = \rho V^2$	modulus of shear elasticity
V	shear wave velocity of the elastic medium
ν	Poisson's ratio of the foundation
P	static horizontal force of alternative loading
$Y(j\omega)$	Fourier's function of microseism
$\phi_{yy(j\omega)}$	the square of transfer function of microseism
$\mu = \delta_{max}/\delta_y$	ductility factor

* Senior Research Officer, Takenaka Technical Research Laboratory, Tokyo
** Research Officer, Takenaka Technical Research Laboratory, Tokyo
*** Associate Professor, University of Tokyo, Faculty of Engineering

1. Foreword

The Tokyo Marine and Fire Insurance Company set up a project to demolish its Old Building, in order to render the land to the proposed new high-rise office building. The Old Building (as referred to T.M.I. Building hereafter) was constructed before the 1923 Kanto Earthquake, survived it, and has been used safely until 1967 with minor repairs and modifications.

On occasion of the demolition, many tests were projected and performed to throw light on the strength and deformation characteristics of the building actually resisted the strong earthquake.

The results of this investigation are of course applicable directly to the structural design of the new building to be constructed on the same site. Furthermore it is believed that this report would provide valuable data for future design of high-rise buildings.

2. Outline of the T.M.I. Building

The construction of this building started on February, 1914, and was concluded on September, 1918. This was the first "building" -- multi-storied office building-- in Japan. The ground floor area was 3412m^2 including annex wings, seven storied without basement, the total floor area being 19537m^2. The plan is shown in Fig. 2. Foundation consisted of compressol type concrete piles topped with concrete footings, connected each other by reinforced concrete footing beams. Exterior frames consisted of built-up steel columns and steel truss girders, covered with brick masonry walls (Fig. 4). Interior frames consisted of built-up steel columns and steel joist girders. Roof and floor systems, consisting of beams and salbs, were made of reinforced concrete.

3. Damages due to 1923 Kanto Earthquake

On September 1, 1923, this building suffered the shock together with its numerous neighbors in Tokyo and suburbs, and survived it. The earthquake originated in the Sagami Bay, south of Tokyo Bay, at about 90Km SSW from the building. The magnitude was 7.9. The earthquake intensity in Tokyo was V (Japan Meteorological Observation Bureau scale).

The official report of the Earthquake is quoted below, as for the damage to the T.M.I. Building.

"This was one of the buildings suffered minor damage. Cracks in the exterior walls extended from first to third story, engraving X marks on the columns, with partial spalling of stone facing or tile facing (Fig. 1). Corners of walls were also damaged. Interior partitions and finishes were partially damaged."

"Floors and walls had no damage. Girders showed some cracks at the haunched ends."

"The inner corner of the building plan showed extensive vertical and inclined cracks."

"Damage to the foundation is not clear but some settlement in general and partial settlement at the north-west corner of the building were noticeable."

4. Object and Scope of Experiments

The test project was divided into loading tests and vibration tests. Loading tests aim at the observation of deformation in the elastic and plastic ranges, load carrying capacity, mode of failure, and deformation at foundations. Vibration tests are for periods of vibration and their change, mode of vibration, and damping characteristics. Static and dynamic analyses accompany these tests.

(a) Horizontal loading, free and forced vibration tests of frame (Block B)

The objective of these tests were to determine stiffness, stress distribution, their changes in the plastic range, and ultimate load carrying capacity and foundation deformation against horizontal loads; natural period, mode and damping of vibration and their changes along with plastic deformation; and finally the safety against earthquakes taking dynamic response analysis into consideration.

The test was performed at Block B, shown in Fig. 2. The entire transverse frame, seven storied without basement, was isolated from other frames in parallel, all the way through from roof to footing, and horizontal loads of equal amount were applied at roof, sixth, fourth, and second floors independently or simultaneously.

At various stages of horizontal loading, free vibration tests were made by the sudden release of horizontal load at the roof, and forced vibration was excited by a vibration generator placed on the seventh floor.

(b) Vertical loading test of floor systems (Portion a.b.)

(c) Vertical loading test of girders (Portion c)

(d) Forced vibration test of a portion of the building (Block A)

(e) Neutralization tests and mechanical tests of materials

Results of these test about item (b) to (e) except (a) are not discribed in this report.

5. Safety against Earthquakes

The current test project concerned with the T.M.I. building which almost safely survived the 1923 Kanto Earthquake. Consequently the investigation as related to the anti-seismic safety of the building received the deepest attention. The investigation was executed in three stages; static loading and vibration tests of a transverse frame, forced vibration tests of a portion of the building, microseism measurement and dynamic analysis of the entire building.

(a) Stiffness, Strength and Dynamic Characteristics of the Frame

i) Outline of Tests

A transverse frame of the building was isolated by cutting all the way from roof to footing. Static horizontal loads were applied both in the positive and negative directions alternately, reactions being rendered from the neighboring portions of the building. Free and forced vibration tests were also carried out. The frame consisted of seven stories and three spans, as whown Fig. 3 to Fig. 4, total height above ground of 26.53m.

At first individual loads were applied separately at each floor so that flexibility coefficients of the frame could be measured. The frame revealed approximately shear type deformation characteristics. The story stiffnesses, or spring constants for vibration analysis, were thus determined experimentally. Secondly, uniform horizontal force was applied to the frame alternately. Due to limitations in the loading set-up, all the seven floors were not subjected to load, however. Loads were applied to the roof, 6th, 4th and 2nd floors, two at each floor, simulating the uniform horizontal loading as much as possible. The direction of loading was reversed at ±48t, ±80t and ±144t, and finally loads were increased to imminent collapse, where the maximum load was again 144t.

The deflection of the frame started to increase rapidly over the elastic deformation at load about 50t, whereby the roof deflection was about 6cm. At load about 100t, the stiffness further decreased and the load reached its maximum (Fig. 5). The final roof deflection was about 58cm. Excluding the effect of rocking measured at foundation, the roof deflection was still 53cm, or about one fiftieth in terms of average column translation angle. After the removal of the ultimate load, the residual deflection at roof was 22cm, showing considerable restoring capacity. The frame also revealed high ductility, as the final deflection was about ten times as much as the deflection at elastic limit, corresponding to load 50t.

Vibration tests were made before, between and after the static horizontal loading. Periods of vibration, modes, and damping were measured. The first natural period was 0.98 sec. before loading test, increased along with stiffness reduction due to loading, and was 1.98 sec. after all the static loadings were completed (Table 1).

ii) Frame Stiffness in the Elastic Range

The stiffness of the frame as determined from test results in the range up to 50t (apparent elastic limit) was about 45 per cent of the calculated stiffness, determined from frame analysis based on the measured section of framing members. The reduction may be attributable to various causes, such as (1) minor damages to the structure due to earthquakes in the past and to demolishing work, (2) partial loss of stiffness due to cracking at low stage of loading, and (3) error in the estimation of modulus of elasticity of materials (normal concrete, lightweight concrete and birck masonry). It is believed that the most important causes would be, first, the overestimation of modulus of elasticity of brick masonry,

loot/cm^2, and second, the presence of preudo elasticity as seen in the test of girders. Structures made of steel and concrete or steel and bricks get flexural cracks at very early stage of loading, leading to stiffness drop, and then show almost linear behavior up to considerably high load.

The natural period of vibration before loading, 0.98 sec., corresponds to the elastic stiffness of uncracked section, and the period after individual loading, 1.29 sec., corresponds to the pseudo elastic stiffness of cracked section. The stiffness reduction associated with this change in period is 57.5 per cent. The above-mentioned stiffness reduction of 45 per cent may be accounted for by this observed reduction and some error in the estimation of modulus of elasticity of brick masonry.

iii) Anti-Seismic Capacity at Elastic Limit

The frame having stiffness as determined from test results was analyzed, and moment distribution and deformation were obtained. The measured horizontal displacements and rotation at column and girder joints agreed satisfactorily with calculated values up to elastic limit of 50t. The calculated steel fiber-stress in the members of third story reached the yield stress at about 50t, which could also be observed in the measured relative displacement. The horizontal load 50t roughly corresponds to static seismic coefficient of 0.1. Within this limit it may be concluded that the frame was elastic, well balanced, and relatively flexible. The foundation of exterior column yielded at the load of 110t. The calculated vertical force at this stage on that foundation was about twice the working load. This bearing capacity of foundation is quite reasonable.

iv) Ultimate Load and Ultimate Deflection

The ultimate load of 144t corresponds to the static seismic coefficient of 0.33, which means a quite severe earthquake.

The ultimate load was calculated by the limit analysis considering yield moment of members determined by the extended reinforced concrete ultimate strength theory (Whitney's theory). The collapse mechanism thus found involved total collapse in the beam yield type for 1st to 4th stories, with upper stories still remaining in the stable state. The yield moment and displacement were analyzed, the ultimate load was 139t according to the potential energy theory $\sum P\delta = \sum M\theta$ (Fig. 6) These findings agreed quite well with observed behavior.

The imminent collapse deflection was calculated using afore-mentioned reduced member stiffness. Since the lower four story collapsed in the beam yield type, which was statically indeterminate within the frame, a considerably complicated procedure was required in the analysis. The calculated roof deflection was 51cm, which was almost equal to the measured deflection of 53cm for the superstructure. The deflected shapes were compared in Fig. 7. Lower stories showed satisfactory agreement, where calculated deflections somewhat exceeded the measured ones. On the other hand calculated deflections were smaller in the upper three stories.

It may be deduced that the final stiffness of columns could be greater than the estimated reduced stiffness, that the final stiffness of girders

in the lower stories was naught as assumed in the analysis, and that the final stiffness of girders in the upper stories was much less than the estimated stiffness.

v) Periods and Modes of Vibration

A series of vibration analysis was made to discuss on the measured data. The relation curve of natural period and its amplitude and the deflection curve of the building in each resonance were shown in Fig. 8 and Fig. 9. The calculated natural period of multi-mass system was 0.89 sec. in the foundamental mode, which was smaller than the measured valve of 0.98 sec, before loading test (Table 1 and 2).

Considering rocking and sway of foundation, the natural period was calculated to treat a structure as shear mass system (Fig. 10).

$$[M]\{\ddot{x}\}+[K]\{x\}=\{0\} \qquad (1)$$

$$[M]=\begin{bmatrix} m_n & & & & \\ & m_{n-1} & & & \\ & & \ddots & & \\ & & & m_1 & \\ & & & & m_0 \\ & & & & & I \end{bmatrix} \qquad (2)$$

$$[K]=\begin{bmatrix} k_n & -k_n & 0 & \cdots & -k_n h_n \\ -k_n & k_n+k_{n-1} & -k_{n-1} & \cdots & k_n h_n - k_{n-1} h_{n-1} \\ & & & & \\ & \cdots & -k_2 & k_2-k_1 \quad -k_1 & k_2 h_2 - k_1 h_1 \\ & \cdots & & -k_1 \quad k_1-k_0 & k_1 h_1 \\ -k_n h_n & k_n h_n - k_{n-1} h_{n-1} & \cdots & k_2 h_2 - k_1 h_1 \quad k_1 h_1 & K_0 - \sum_1^n k_T h_T^2 \end{bmatrix} \qquad (3)$$

The virtual mass m_0 was recognized the function of a ground wave's frequency in general, now was only placed to the mass of foundation. The moment of inertia of foundation I was defined by

$$I = I_0 + \sum mH^2 \qquad I_0 = \frac{\sum m_1 (2a)^2}{12} \qquad (4)$$

The spring constants of horizontal and rotational stiffness of a rigid foundation were shown assuming Boussinesq distribution of reaction on the surface of the foundation.

$$k_o = \frac{8aG}{2-\nu} \qquad (5)$$

$$k_\theta = \frac{8a^3G}{3(1-\nu)} \qquad (6)$$

Estimating the shear wave velocity of the elastic medium was 300m/sec. the first natural period was 0.96 sec. The periods associated with higher modes were very little affected by rocking and sway, and generally coincided with measured periods except for some difference in case of second period (Fig. 11). This finding and the property of measured mode indicated that this frame could be idealized to shear type vibrational mode.

Along with static loading cycles, the measured period increased gradually, up to the final valve of 1.98 obtained after ultimate load (Table 1). This change approximately corresponded to the stiffness change due to plastification. The period after ultimate loading was 1.98 sec. by free vibration test, 1.55 sec. by forced vibration test, and 1.20 sec, by microseism analysis. The associated amplitude was smaller in this order. (This would indicate a non-linear force-displacement relation of the structure in the plastic range.

vi) Damping

The damping coefficient measured before the loading tests was 3.6% of critical damping for the first mode, and the damping coefficients associated with higher modes were rather small. (Fig. 12). This suggests that the damping characteristics of this frame cannot be approximated by the conventional internal damping which increases in proportion to the natural frequency.

Along with the increase in the first natural period for later cycles of loading, damping increased up to 7% after the ultimate loading (Table 3). The equivalent viscous damping obtained from the area of hysteresis curve by static loading roughly coincided with the measured damping, except for ultimate loading (Table 4). The very small amplitudes associated with the vibration tests would explain the reason for this difference.

If the damping matrix is a linear combination of the mass matrix and the stiffness matrix, the damping matrix may be written as

$$[C] = \alpha [M] + \gamma [K] \qquad (7)$$

where α and γ are real constants.
According to Caughey damping series, the relation of the frequency and damping over high mode could be expressed in the following form:

$$[M]^{-\frac{1}{2}}[C][M]^{-\frac{1}{2}} = \sum_{l=0}^{n=l} \beta_l \left([M]^{-\frac{1}{2}}[K][M]^{-\frac{1}{2}} \right)^l \qquad (8)$$

As the damping coefficients and frequencies were known from vibration test, Eq(8) could be expressed in the following form

$$[\beta_0, \beta_1, \cdots\cdots \beta_{n-1}] \begin{Bmatrix} 1 \\ \lambda \\ \lambda_j^2 \\ \vdots \\ \lambda_j^{n-1} \end{Bmatrix} = 2h_j \lambda_j^{\frac{1}{2}} \quad (j=1\sim n) \qquad (9)$$

Damping factors Cij of (2 -1) numbers were computed by the vibrational mode as shown:

$$\begin{bmatrix} \psi_{j5} & \psi_{j4} & 0 & 0 & 0 & 0 & 0 & 0 & 0 \\ 0 & \psi_{j5} & \psi_{j4} & \psi_{j3} & 0 & 0 & 0 & 0 & 0 \\ 0 & 0 & 0 & \psi_{j4} & \psi_{j3} & \psi_{j2} & 0 & 0 & 0 \\ 0 & 0 & 0 & 0 & 0 & \psi_{j3} & \psi_{j2} & \psi_{j1} & 0 \\ 0 & 0 & 0 & 0 & 0 & 0 & 0 & \psi_{j2} & \psi_{j1} \end{bmatrix} \begin{Bmatrix} C_{55} \\ C_{45} \\ C_{44} \\ C_{43} \\ C_{33} \\ C_{32} \\ C_{22} \\ C_{21} \\ C_{11} \end{Bmatrix} = \begin{Bmatrix} 2m_5 h_j \psi_{j5} \omega_j \\ 2m_4 h_j \psi_{j4} \omega_j \\ 2m_3 h_j \psi_{j3} \omega_j \\ 2m_2 h_j \psi_{j2} \omega_j \\ 2m_1 h_j \psi_{j1} \omega_j \end{Bmatrix} \quad (1($$

β_j and the damping matrix of Cij were solved.

$$\beta_0 = 2.725\times10^{-1}$$
$$\beta_1 = 3.483\times10^{-3}$$
$$\beta_2 = -3.390\times10^{-6}$$
$$\beta_3 = 1.012\times10^{-9}$$

$$[C] = \begin{bmatrix} 0.29 & -0.16 & 0 & 0 & 0 & 0 & 0 \\ -0.16 & 0.35 & -0.16 & 0 & 0 & 0 & 0 \\ 0 & -0.16 & 0.37 & -0.19 & 0 & 0 & 0 \\ 0 & 0 & -0.19 & 0.39 & -0.19 & 0 & 0 \\ 0 & 0 & 0 & -0.19 & 0.34 & -0.13 & 0 \\ 0 & 0 & 0 & 0 & -0.13 & 0.21 & -0.06 \\ 0 & 0 & 0 & 0 & 0 & -0.06 & 0.08 \end{bmatrix} \qquad (11)$$

(b) Dynamic Characteristics of the Entire Building

i) Dynamic Characteristics in the Elastic Range

As vibration test was not carried out for the entire building owing to machinery limitation, the natural periods and modes were estimated from the microseism analysis and structural analysis based on the measured cross-section of members.

Microseism was measured at the central wing and west wing of the building, simultaneously on the roof and ground floors, both in NS and EW

directions The displacement data and its autocorrelation were subjected to Fourier analysis. (Fig. 13) The spectrum of the roof data, and the spectral ratio of the roof and ground data were used to estimate the natural period. As to the latter, the spectral ratio of the roof and ground displacement theoretically gives the transfer function, whereas the spectral ratio of the autocorrelation gives the square of the transfer function. Thus their peak values theoretically correspond to the dynamic property of the superstructure.

The analysis resulted in the estimated first period of 0.43 to 0.48 sec. in the NS direction and 0.40 to 0.45 sec. in the EW direction, both including rocking effect. (Table 5). The period associated with superstructure only was generally smaller, but the difference was at most 0.02 sec., indicating a negligible effect. There was no difference in the periods of central and west wings, so that the building seemed to vibrate at its entirety.

The stiffness, calculated by the frame analysis, consisted of walled frame stiffness of exterior frames and open frame stiffness of interior frames. Assuming the modulus of elasticity of brick masonry of $100t/cm^2$, the former occupied about 85 per cent of total stiffness. The calculated periods of vibration were 0.44 sec. in the NS direction, and 0.38 sec. in the EW direction.

As was stated several times previously, the actual modulus of elasticity of brick masonry was believed to be less, loading to the increased periods, resulting better agreement with microseism analysis.

ii) Restoring Force Characteristics

The current test project originally included the load test of walled frame of steel and brick masonry, but it had to be omitted according to various limitations. The restoring force characteristics had to be estimated from available literature.

The brick masonry wall was regarded as completely elasto-plastic shear body with yield shear strain of 0.50×10^{-3}, and failure at ductility factor of 4.

The walled frame deforms in bending as well as in shear. The ratio between column translation angle and shear strain was calculated for typical walled frames of the Building. The average of the ratio was 3, which determines the restoring force characteristics of walled frames.

The open frame may be regard as elastic in the range considered. Combining them according to their shares in the stiffness, a bi-linear elasto-plastic restoring force characteristics were obtained for the entire building as shown in Fig. 14.

6. Response and Resistance to Earthquake of the Building.

(a) Response to Earthquake of the Frame

The earthquake response of the frame, which was subjected to series of

tests and analyses, was calculated for El Centro 1940 NS record with maximum ground acceleration 330 gal. The objective of the response analysis was two fold; first to study the effect of vibration characteristics of the frame determined in the test, such as relatively low damping coefficients for higher modes, or rocking and sway at foundation; and second to correlate the maximum response and static test by analyzing the multi-mass model with realistic restoring force characteristics.

A vibratory system having internal damping and another system having damping characteristics observed in the test were analyzed and compared. The latter showed 20% greater response at upper stories than the internal damping system, but the difference was trivial at lower stories. The difference at upper stories is evidently attributable to the damping coefficient in higher modes, which increases in proportion to natural frequency in case of internal damping.

A system considering rocking and sway at foundation resulted in the response 20 to 40% greater than the system with fixed base (Table 6, Fig.15). This can be explained by longer natural period and apparent decrease in damping coefficient.

The elasto-plastic response of systems having yield seismic coefficient of about 0.15 at the first story and various plastic gradient were analyzed. The maximum responses showed considerable decrease in general from linear responses. The minimum response was obtained when the stiffness in the plastic range was assumed to be 40% of elastic stiffness, which best simulated the observed behavior of the frame. When the smaller plastic gradient was assumed, the lower stories got greater deformation. This concentrated plastic deformation decreased the response value of upper stories, but the total deformation was still greater.

In the analysis the elastic stiffness was held constant up to the yield point, whereas cracking appeared in the test at very low load. Owing to this difference in the procedure of analysis, the direct comparison of response and test results was not feasible.

However, it should be noted that Cases 5 and 8, which were based on the yield seismic coefficient of 0.15 and realistic elasto-plastic restoring force function, resulted in the base shear coefficient of about 0.245 for the ground motion with maximum acceleration 0.33g. According to the response analysis, the ductility factors at 1st, 2nd and 3rd stories were 1.5 to 2.5, and upper stories generally remained in the elastic range. Evidently this is within the safety limit in terms of strength as well as deformation. The elastic (linear) analysis completely failed to predict this conclusion. The importance of non-linear analysis based on the realistic assumption should be noted.

(b) Response to Earthquake of the Entire Building

The non-linear vibratory systems constructed on the clues of microseism observation and available literature were subjected to El Centro 1940 NS earthquake 330 gal.

Three non-linear systems were analyzed for each of NS and EW directions, where variables were stiffness and plastic stiffness reduction. The elastic stiffness was established corresponding to modulus of elasticity of brick masonry of 1.0×10^5, 0.7×10^5, 0.5×10^5, kg/cm^2, and accompanying plastic gradient was 0.15, 0.30, 0.30, respectively, of the elastic stiffness. The yield point was set at the column translation angle of 1.5×10^{-3} (Table 7).

The response of Case 1, the system with shortest natural period of T=0.38 sec. and low plastic gradient of 0.15, differed entirely from all other cases as shown in Fig. 16. This could be an example of the singular response of multi-mass system, having short period and low plastic stiffness.

All other cases had similar response. The plastification was intensive in 1st, 2nd and 3rd stories, especially in the 2nd story. It is inferred that Case 5 and Case 6, corresponding to the lowest elastic stiffness and highest plastic gradient assumed, would represent the best approximation of actual condition. In these cases the ductility factors at 2nd story were 4 in NS direction and 3 in EW direction, and upper stories (4th story and above) remained in the ductility factor of 2 or less. The base shear in these cases were 6080t in NS direction and 7000t in EW direction, or base shear coefficient of 0.39 and 0.45 respectively.

As the record of 1923 Kanto Earthquake was not available, the above-mentioned findings may not be directly extended to actual response to Kanto Earthquake. Nevertheless, it is very interesting to note the surprising similarity to the actual damage as outlined in Chapter 3. The building suffered the damage corresponding to ductility factor of 4 or more from the Kanto Earthquake, and survived it as a total structure, and was used safely for 50 years. The building showed ductility of 4 against El Centro Earthquake in the analysis, the wave most commonly used in the current dynamic design of tall buildings. This would suggest that allowable ductility factor of 4 for El Centro Earthquake could be a safe criterion for earthquake resistant design.

Acknowledgement

We would express to thank Prof. H. Umemura, Prof. Y. Osawa and Mr. M. Itoh, Tokyo University. Also we appreciate Tokyo Marine and Fire Insurance Company.

Reference:

Nielsen, N.N. : Theory of Dynamic Tests of Structure
The Shock and Vibration Bulletin
U.S. Naval Research Laboratory, Jan. 1966.

Whitman, R.V. : Analysis of Foundation Vibrations. Proceedings of a Symposium organized by the British National Section of ISEE. London, April, 1965.

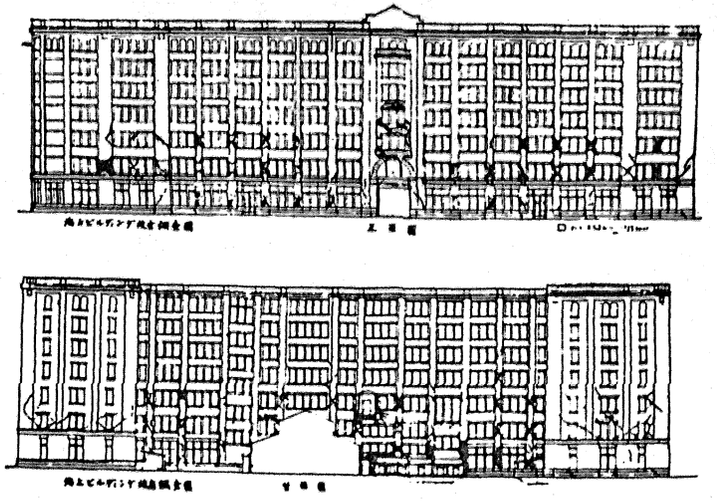

Fig.1. Damages to the Building due to 1923 Earthquake

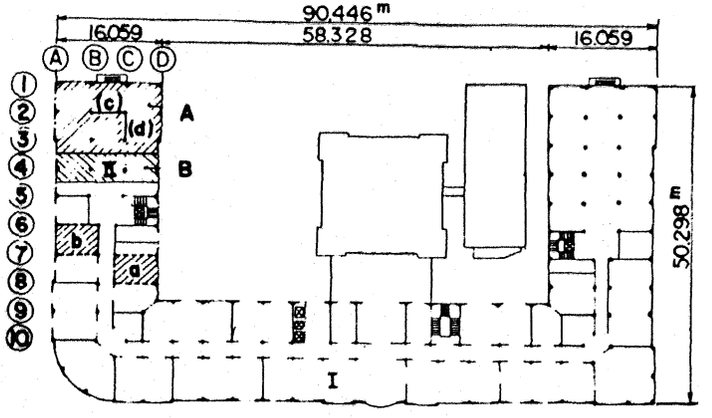

Fig.2. Locations of Test Structures for the Current Test Project

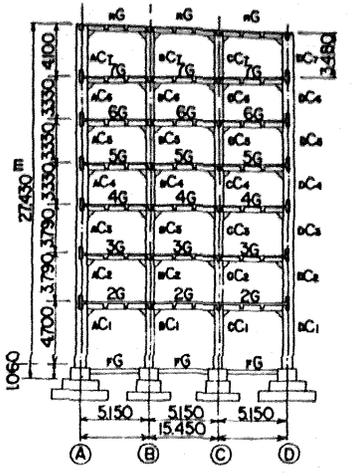

Fig.3. Elevation of the Test Frame

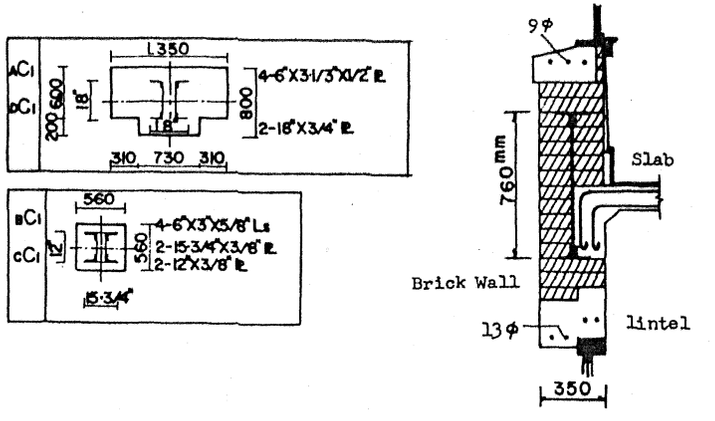

Fig.4. Section of Framing Members (First Floor) and Exterior Wall

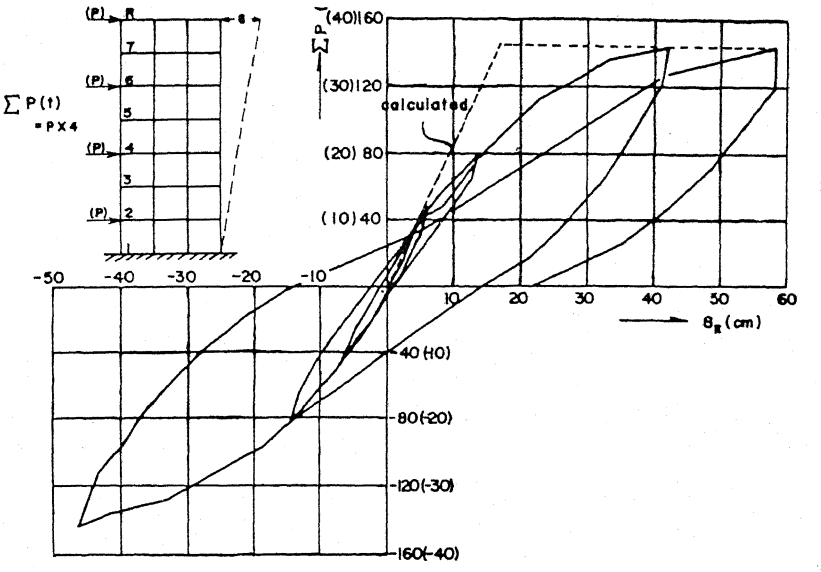

Fig.5. Deflection at R-Floor under Total Loading

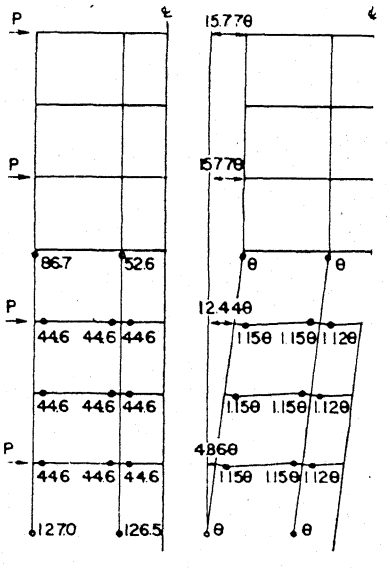

Fig.6. Collapse Mechanism of the Frame

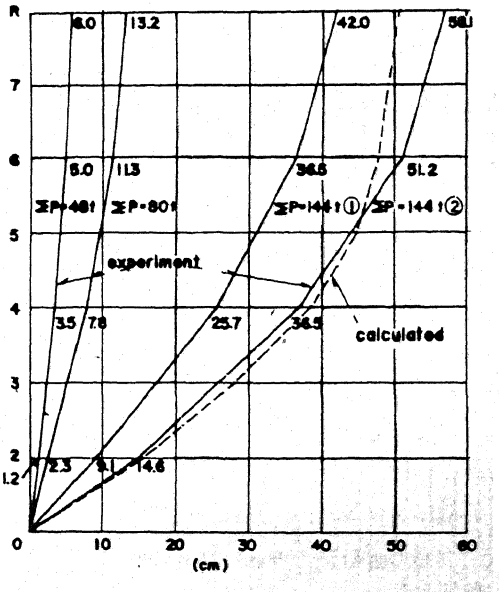

Fig.7. Mode of Deflection under Total Loading (Measured vs. Calculated)

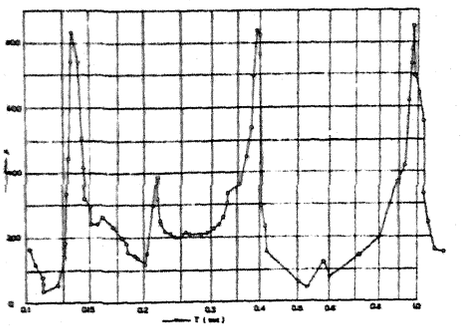

Fig.8. Resonance Curve at R-Floor (Test No.1)

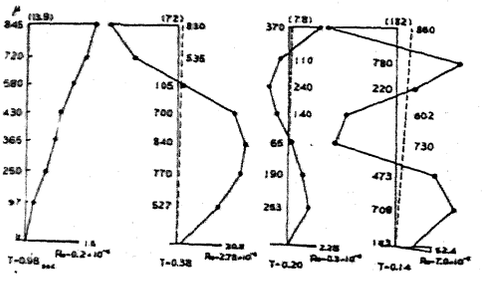

Fig.9. Mode of Vibration (Test No.1)

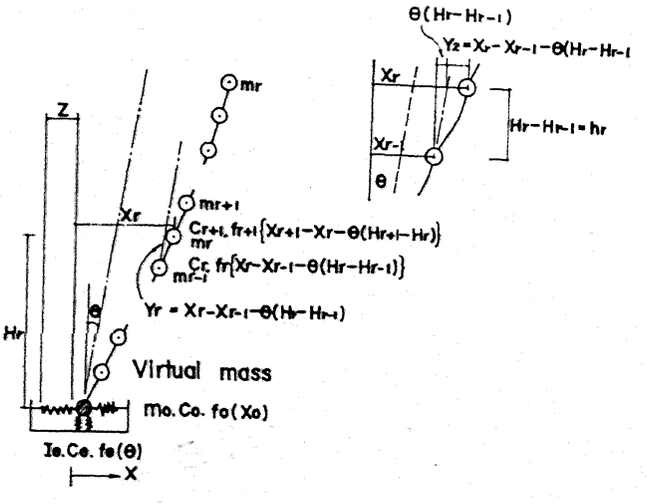

Fig.10. Multi-mass and Spring System

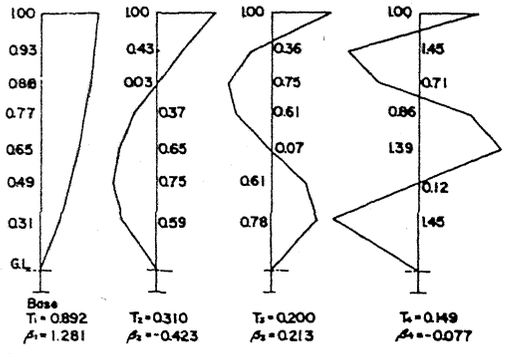

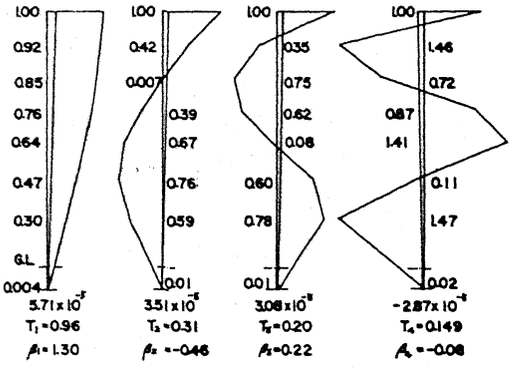

Fig.11. Mode of Vibration (Test No.1)

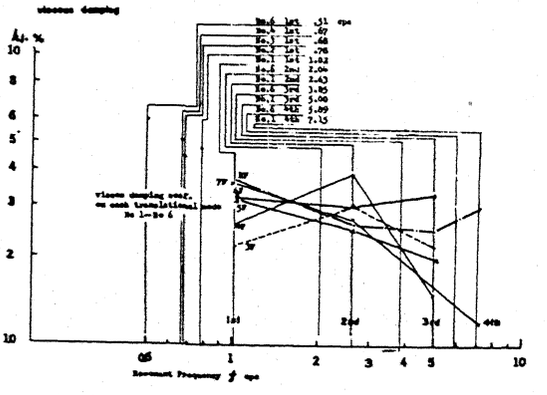

Fig.12. Relation between Frequency and Damping Coefficient

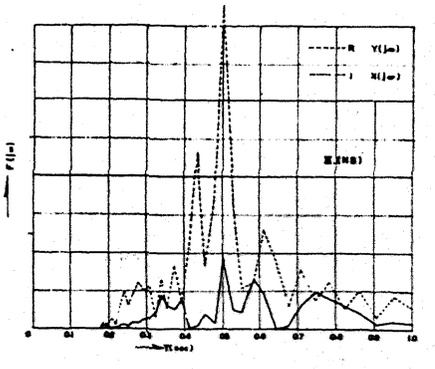

Fig.13. Fourier Spectrum F(jw) for II point in NS Direction

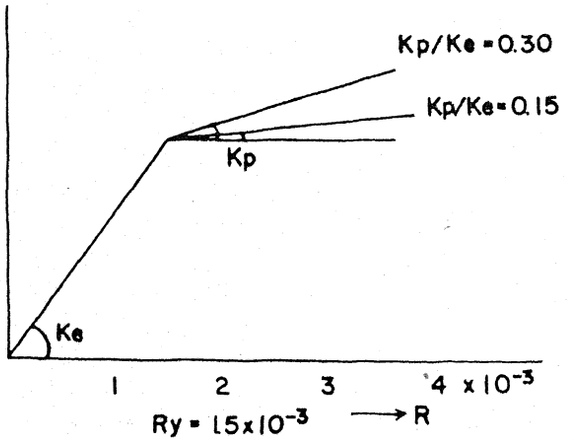

Fig.14. Assumption of Restoring Force Characteristics of the Building

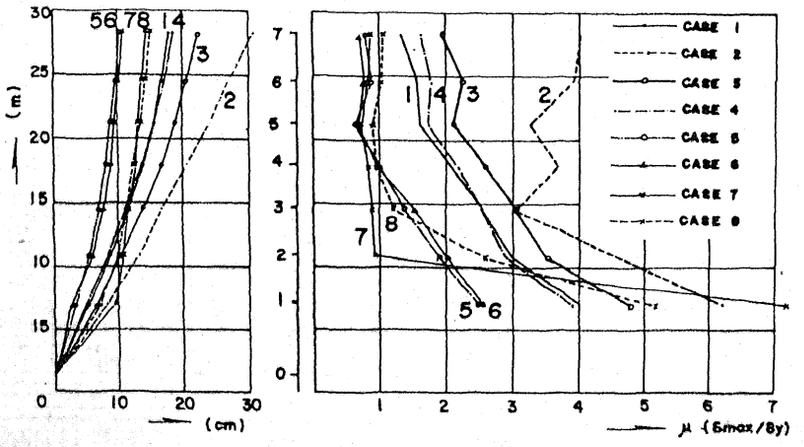

Fig.15. Maximum Response Deflection and Ductility Factor for the Frame

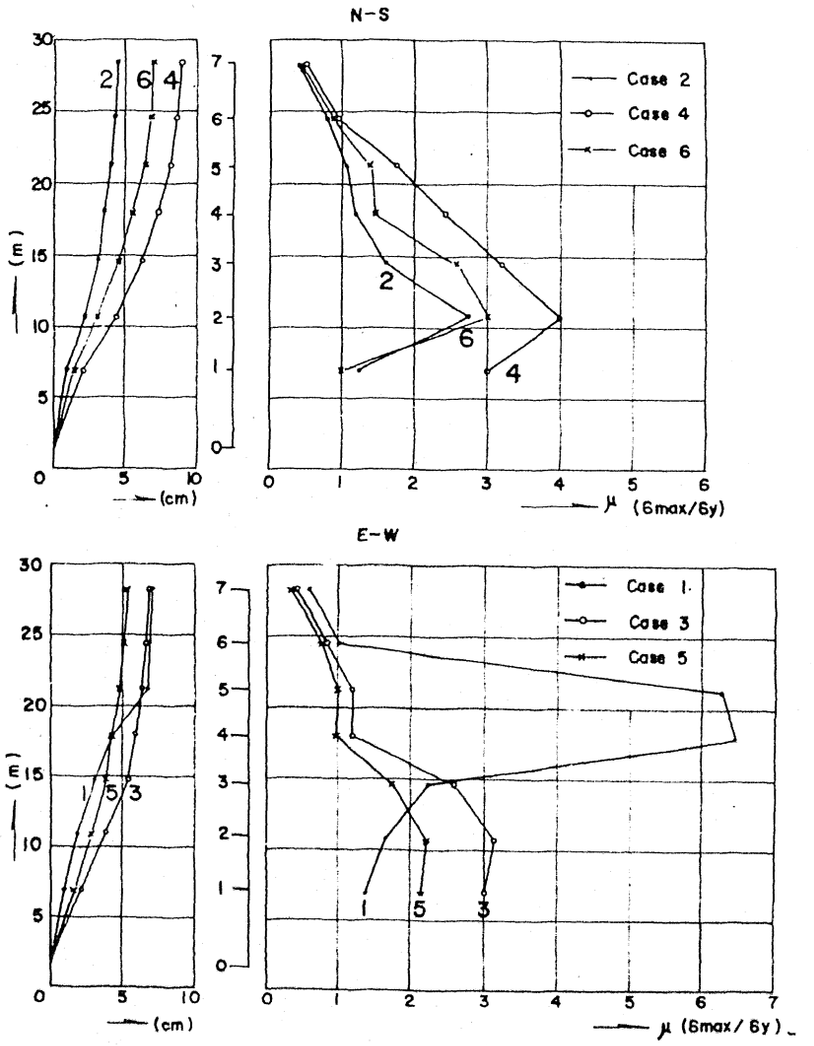

Fig.16. Maximum Response Deflection and Ductility Factor for the Building

Table 1. Static Loading Stage and Fundamental Period of Vibration after each stage

	№ 1	№ 2	№ 3	№ 4	№ 5	№ 6
Tests of vibration	Forced vibration	Free vibration test			Forced vibration	Free vibration
Condition of static loading	before loading	R·6F 10t 4.2F 20t	after ± 48 t	after ± 80 t	after maximum load + 144t	
1st Periods (sec)	0.98	1.29	1.47	1.49	(1.55)	1.98

Table 2. Measured and Calculated Periods

Mode of vibration	1st	2nd	3rd	4th
№1 Measured periods	0.98	0.38	0.20	0.14
" Calculated values	0.89	0.31	0.20	0.15
" included rocking sway	0.96	0.31	0.20	0.15
№2 Measured periods	1.29 (Free vibration test)			
" Calculated values	1.19	0.43	0.27	0.21
№5 Measured periods	1.55 (1.98)	0.49	0.26	0.17

( ) : result of free vibration test

Table 3. Damping Coefficient

Tests	№1 ※	№2	№3	№4	№5 ※	№6
Viscous damping (%)	3.6	4.8	4.5	5.1		7.0
1st periods (sec)	0.98	1.29	1.47	1.49	(1.55)	1.98

※ Forced vibration test

Table 4. Equivalent Viscous Damping Coefficient as Estimated from Hysteresis Curves

Condition of static loading	after ±48t	after ±80 t	after ±144t	maximum +144t
Base shear coef	0.112	0.186	0.335	0.335
RF (α_0)( )cm	3.8(7.3)cm	5.4 (14.5)	14.4(46.5)	13.4(58.0)
7F	4.3(6.5)	5.2 (13.0)	14.4(43.5)	14.2(54.5)

( ) : Maximum displacements of static loading

Table 5. List of Fundamental Periods

	Max Times.	Fourier's Y(jω)		Autocorrelation's $\Phi_{yy}(j\omega)$	
	I	I	II	I	II
NS	0.41 sec	0.47 sec (0.46 sec)	0.48 sec (0.44 sec)	0.43 sec (0.43 sec)	0.45 sec (0.45 sec)
EW	0.36 sec	0.45 sec (0.43 sec)	0.45 sec (0.43 sec)	———	0.40 sec (0.40 sec)

( ) spectral ratio

Table 7. Stiffness (Spring Constants) for Each Case Considered

CASE		I	II	III	IV	V	VI	
E(brick)		1.0×10^5 kg/cm²		0.7×10^5 kg/cm²		0.5×10^5 kg/cm²		Xy cm
i	Mi t·sec²/cm	Ki (t/cm) (EW)	(NS)	Ki (t/cm) (EW)	(NS)	Ki (t/cm) (EW)	(NS)	
7	2.02	1.27 x10	0.835x10	0.898 x10	0.59x10	0.635x10	0.418x10	0.57
6	2.24	1.33	0.91	0.94	0.644	0.665	0.455	0.50
5	2.19	1.34	0.95	0.946	0.671	0.67	0.475	0.50
4	2.21	1.63	1.08	1.15	0.764	0.815	0.540	0.50
3	2.41	1.32	1.02	0.934	0.721	0.66	0.510	0.57
2	2.40	1.38	1.03	0.975	0.729	0.69	0.515	0.57
1	2.41	1.23	1.07	0.87	0.757	0.615	0.535	0.71
K_p/K_e		0.15	0.15	0.30	0.30	0.30	0.30	
T_1		0.384	0.436	0.456	0.521	0.543	0.620	

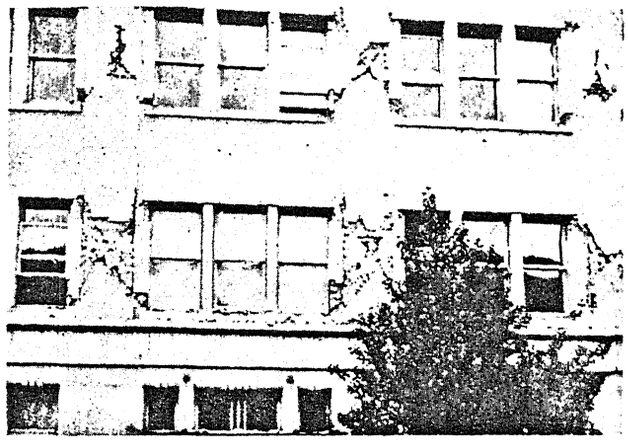

Photo-1 Damages to the Building due to 1923 Earthquake

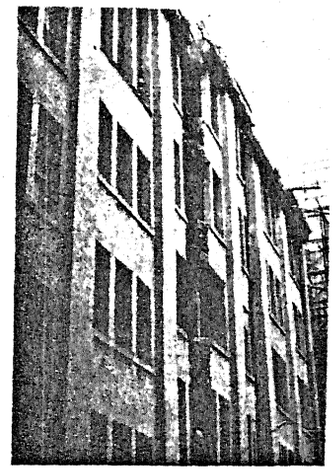

Photo-2 Deformation of Test Frame at Ultimate

Table 6. Elastic and Elasto Plastic Response of the Frame for Various Conditions

Periods (SEC).				case	1	2	3	4	5	6	7	8
	Measured	Calculated			Fix		Rocking Sway		Fix			Rock.Sway
Tj		Fix	Rock.Sway	hj	$\propto \omega_j$	Measured	$h_j=3.2$ $C_0.C_\theta$	$h_j=0$ $C_0.C_\theta$	Calculated (Linear to ω_j)			$h_j=3.2$ $C_0.C_\theta$
T_1	0.98	0.89	0.96	h_1	3.2 %	3.2 %	2.5 %	0.058 %	3.2 %			2.5 %
T_2	0.38	0.31	0.31	h_2	9.2	3.0	9.2	0.044	9.2			9.2
T_3	0.20	0.20	0.20	h_3	14.2	2.2	14.2	0.036	14.2			14.2
T_4	0.14	0.15	0.15	h_4	19.2	2.0	19.2	0.033	19.2			19.2

						Max Relative Displacement (cm)							
	Mass	Spring	Displ.	Cl	Height	Linear				Non-Linear (K_D/K_θ)			
j	Mj(t·sec²/cm)	Kj (t/cm)	Xyj(cm)	Cj(t·sec/cm)	Hj(m)	case 1	2	3	4	5 (0.4)	6 (0.25)	7 (0)	8 (0.4)
7	0.0554	40.20	0.92		28.28	1.25 cm	1.50 cm	1.82 cm	3.69 cm	0.72 cm	0.98 cm	0.78 cm	0.62 cm
6	0.0620	83.08	0.76		24.49	1.20	1.35	1.71	2.97	0.65	0.80	0.64	0.59
5	0.0609	87.60	1.04		21.19	1.68	1.81	2.20	3.40	0.65	0.94	0.75	0.67
4	0.0594	88.98	1.02		17.89	2.11	2.20	2.63	3.75	1.00	0.98	0.86	0.95
3	0.0666	77.35	1.15		14.59	2.93	2.95	3.52	3.51	1.59	1.44	1.05	1.79
2	0.0660	77.35	1.11		10.80	3.30	3.24	3.88	5.04	2.10	2.89	1.03	2.24
1	0.0680	49.86	1.35		7.01	5.44	5.29	6.52	8.38	3.35	7.02	9.71	3.46
0	0.1210	310.0	∞	26.4	—			0.087	0.116				0.031
I	82×10^4	441×10^6	∞	414×10^3	—			1.28×10^{-3}	1.67×10^{-3}				0.44×10^{-3}